Environment International 127 (2019) 78–84

Contents lists available at ScienceDirect

Environment International

journal homepage: www.elsevier.com/locate/envint

Increased secondary aerosol contribution and possible processing on polluted winter days in China

Yichen Wang[a,b], Ji Chen[c], Qiyuan Wang[b,d,*], Quande Qin[a,**], Jianhuai Ye[e], Yuemei Han[b], Li Li[a], Wei Zhen[a], Qiang Zhi[f], Yixuan Zhang[b], Junji Cao[b,d,*]

[a] College of Management, Shenzhen University, Shenzhen 518060, China
[b] Key Lab of Aerosol Chemistry and Physics, SKLLQG, Institute of Earth Environment, Chinese Academy of Sciences, Xi'an, China
[c] Aarhus University Centre for Circular Bioeconomy, Department of Agroecology, Aarhus University, BlichersAllé 20, 8830 Tjele, Denmark
[d] CAS Center for Excellence in Quaternary Science and Global Change, Xi'an 710061, China
[e] School of Engineering and Applied Sciences, Harvard University, Cambridge, MA 02138, USA
[f] School of Government Administration, Central University of Finance and Economics, China

ARTICLE INFO

Handling Editor: Hefa Cheng

Keywords:
Secondary aerosols
Aqueous-phase reactions
Photochemical reactions
Polluted days
Winter

ABSTRACT

China experiences severe particulate pollution, especially in winter, and determining the characteristics of particulate matter (PM) during pollution events is imperative for understanding the sources and causes of the pollution. However, inconsistencies have been found in the aerosol composition, sources and secondary processing among reported studies. Modern meta-analysis was used to probe the PM chemical characteristics and processing in winter at four representative regions of China, and the first finding was that secondary aerosol formation was the major effect factor for PM pollution. The secondary inorganic species behaved differently in the four regions: sulfate, nitrate, and ammonium increased in the Beijing–Tianjin–Hebei (BTH) and Guanzhong (GZ) areas, but only nitrate increased in the Pearl River Delta (PRD) and Yangtze River Delta (YRD) regions. The increased production of secondary organic aerosol (SOA) was probably caused by aqueous-phase processing in the GZ and BTH regions and by photochemical reactions in the PRD. Finally, we suggest future AMS/ACSM observations should focus on the aerosol characteristics in rural areas in winter in China.

1. Introduction

Particulate pollution influences climate, public health, and ecosystems, and therefore, particulate matter (PM) is a major ecological concern (Fu and Chen, 2017; Fuzzi et al., 2015; Lelieveld et al., 2015). Widespread PM pollution often occurs in China during the winter, and the impacts of air pollutants are of particular concern because the concentrations often exceed the levels established in health guidelines, and there is expected to be continued reliance on fossil fuels (Zhang et al., 2012). Aerosol Chemical Speciation Monitors (ACSMs) and Aerosol Mass Spectrometers (AMSs) have been frequently deployed in China to investigate the mechanisms that cause particulate pollution (Li et al., 2017; Pratt and Prather, 2012). These devices are used for real-time tracking of the mass concentrations of non-refractory chemical species, including organic aerosol (OA), sulfate, nitrate, ammonium and chloride. Among these species, the sum of sulfate, nitrate and ammonium is regarded here as the secondary inorganic aerosol (SIA).

The OA often accounts for the largest fraction of submicron aerosols in China, and the sources for OA are varied and complex (Li et al., 2017; Tao et al., 2017). Recognizing the importance of identifying and quantifying OA, researchers have applied the Multilinear Engine (ME-2) and positive matrix factorization (e.g., Huang et al., 2014; Jimenez et al., 2009) for these purposes. Typically, the OA is separated into two groups: the oxygenated OA (OOA) and primary OA (POA). Lanz et al. (2007) and Zhang et al. (2007) have demonstrated OOA to be mainly composed of secondary OA (SOA). Additionally, POA can be separated into organic aerosols from cooking (COA), coal combustion (CCOA), biomass burning (BBOA), and traffic (HOA) (Wang et al., 2017a; Lanz et al., 2007; Li et al., 2017).

Increases in relative humidity (RH) lead to more aerosol liquid water, which determines the size of the "reactor" in which the aqueous-phase formation of secondary aerosols can occur (Duplissy et al., 2011; Ervens et al., 2011). Thus, correlation analysis of secondary aerosols and RH has been used as an indicator of possible aqueous-phase

* Corrresponding authors at: Key Lab of Aerosol Chemistry and Physics, SKLLQG, Institute of Earth Environment, Chinese Academy of Sciences, Xi'an, China
** Corrresponding author.
E-mail addresses: wangqy@ieecas.cn (Q. Wang), qinquande@gmail.com (Q. Qin), cao@loess.llqg.ac.cn (J. Cao).

https://doi.org/10.1016/j.envint.2019.03.021
Received 22 October 2018; Received in revised form 9 March 2019; Accepted 9 March 2019
Available online 23 March 2019

reactions (Huang et al., 2019; Sun et al., 2013b; Xu et al., 2016). Increased solar radiation (SR) promotes photochemical reactions that lead to the formation of secondary aerosols (Hallquist et al., 2009; Hartikainen et al., 2018; Walser et al., 2007, 2008; Zhang et al., 2014a), and therefore, the intensity of SR has been used as an indicator of photochemical reactivity in the atmosphere (Hallquist et al., 2009; Wang et al., 2017a).

The mass loadings of aerosol chemical constituents, especially organic species, can undergo substantial variations during particulate pollution events (Huang et al., 2014). "Major effect factor" refers to the aerosol composition or organic sources that have increased mass fractions during pollution events (Huang et al., 2014). Characterization of the major chemical species is useful for understanding the mechanisms that cause the problems at specific sites because the pollution events are driven by different types and organic sources at different cities in China (e.g., Huang et al., 2014; Tao et al., 2017; Zhang et al., 2017). For example, sulfate was the major effect factor in Xi'an in the Guanzhong (GZ) region where its mass fraction increased by 6% in pollution events (Wang et al., 2016). In contrast, in Guangzhou in the Pearl River Delta (PRD) area, the nitrate mass fractions increased with the PM_1 mass concentrations (Qin et al., 2017). On polluted days, a 10% increase in the contribution of biomass burning OA (BBOA) to OA was noted in Xi'an (Wang et al., 2017b), and OOA mass fractions in OA increased by approximately 9% in Beijing (Elser et al., 2016).

Furthermore, the major effect factors identified for pollution events in the same city have varied among studies. In Beijing, for example, Hu et al. (2016) found that high pollution periods were characterized by an increase in the organic aerosol fraction; by contrast, SIA—including SO_4^{2-}, NO_3^-, and NH_4^+—formation was noted to increase by Sun et al. (2014). Moreover, Sun et al. (2013a) reported an increase in coal combustion–related OA in Beijing, but Elser et al. (2016) observed enhanced SOA formation.

While the characteristics of inorganic aerosols in China have been relatively well characterized (Cheng et al., 2016; Wang et al., 2016), the aqueous phase and photochemical processing of SOA, and the importance of these particles for particulate pollution, remain relatively uncertain (Zhang et al., 2015). Further, different mechanisms have been invoked to explain the formation of SOA. In Beijing, for example, Hu et al. (2017) reported that aqueous-phase reactions dominated OOA formation, but Sun et al. (2013b) reported that aqueous-phase processing did not cause large increases in OOA. Such inconsistency challenges our understanding of pollution formation mechanism in China. Synthesizing the results from pollution studies can help resolve the inconsistencies in the literature, and meta-analysis is a quantitative approach for doing this (Glass, 1976).

One of the fundamental goals of a meta-analysis is to generalize outcomes from multiple studies to obtain a more comprehensive understanding than what one could learn from an individual study (Gurevitch et al., 2018). Most meta-analysis studies fall into two categories (1) methods for combining probabilities and (2) modern meta-analyses. The former of these types, combines statistical results from numerous studies based on exact values to provide an overall assessment of significance—these methods have been used to synthesize the characteristics of aerosol species in China (Fontes et al., 2017; Tao et al., 2017; Zhang et al., 2017), Europe (Lanz et al., 2010; Viana et al., 2008), and India (Banerjee et al., 2015). Some investigators have used an approach that involved averaging values to synthesize the salient aerosol characteristics instead of focusing on aerosol characteristics for days with heavy pollution. Using averages for summarization purposes can be difficult, however, because the included studies often use different sampling procedure or observation periods, and short-term studies frequently report larger and more variable effects than those reported for long-term studies. This means that the short-term studies are more likely to suffer from random noise and extreme values (Button et al., 2013), and therefore, weighting of some form is often desirable.

In addition, effect-size variances are a function of sample size; therefore, large-sample theory posits that studies that have larger sample sizes would exhibit lower variances and would thus provide more accurate estimates of the true effect size of a population (Hedges, 1994). To account for this, modern meta-analyses typically employ weighted averages for estimating the cumulative effect size for a group of studies: in practice, the weight for a single study is usually taken as the reciprocal of the sampling variance. Small sample sizes also are more likely to violate basic distribution-based assumptions, such as normality. Resampling techniques, for example bootstrapping, in modern meta-analyses are useful for assessing the significance of the meta-analytical metrics (Hedges, 1994).

Modern meta-analyses have been successfully used in our research group to probe the effects of air pollution on ecosystems (Chen et al., 2015, 2017, 2018a). Here, the results from regional distributions of 23 AMS/ACSM studies were synthesized through a meta-analysis to characterize the variations in aerosol characteristics and thereby determine the major effect factor of PM pollution during winter. Relationships between OOA and meteorological parameters (i.e., relative humidity [RH] and solar radiation [SR]) were evaluated to investigate the chemical processing of SOA in four representative regions in China. To the best of our knowledge, this is the first time that modern meta-analysis has been used to probe the variations in aerosol characteristics on polluted days.

2. Materials and methods

2.1. Data sources

Studies based on AMS/ACSM measurements in China started in 2006, and they have continuously increased in number (Li et al., 2017). We sought out journal articles with publication dates prior to February 2019 on the Web of Science platform (http://apps.webofknowledge.com/). In the literature search, the keywords and phrases used were as follows: (1) "particulate matter" OR "aerosol" OR "$PM_{2.5}$" OR "PM_1," AND (2) "China" OR "Chinese," AND (3) "Aerosol Chemical Speciation Monitor" OR "ACSM" OR "Aerosol Mass Spectrometer" OR "AMS." Studies were chosen on the basis of the following conditions:

(1) Only measurements taken during winter were included.
(2) Only measurements taken in urban environments were included.
(3) Source apportionments of OA were reported.
(4) If an article reported more than one measurement from multiple study sites, as done by Elser et al. (2016) and Huang et al. (2014), each measurement was considered an independent study.
(5) If multiple sets of measurements were made at the same site in the same year (Elser et al., 2016; Sun et al., 2015; Huang et al., 2014; Hu et al., 2017; Sun et al., 2014, and Zhang et al., 2014b)—each measurement period was treated as an independent study.
(6) If the organic source apportionment results did not include non-negligible biomass burning sources in addition to coal burning in Northern China, the source apportionment results were excluded (i.e., Hu et al., 2017; Sun et al., 2013a, 2014; Wang et al., 2015; Zhang et al., 2016a, 2016b).

We selected 23 articles on the basis of the aforementioned conditions (Table S1). As shown in Fig. S1, most of the measurements were conducted in four representative regions in China.

2.2. Data collection

For each chosen study, we documented the study site, study period, aerosol type (PM_1: aerodynamic diameter $\leq 1\,\mu m$ or $PM_{2.5}$: aerodynamic diameter $\leq 2.5\,\mu m$), and aerosol species mass concentrations (both inorganic components and organic sources in $\mu g\,m^{-3}$) over the entire campaign period. We used the Engauge Digitizer 2.24 (http://markummitchell.github.io/engauge-digitizer/) for digitizing and

extracting the data from time-series graphs of chemical species, organic sources, and meteorological parameters. The extracted time-series data were further averaged to obtain daily averages. Details regarding data collection are provided in the supplementary material.

2.3. Effect size calculation

Effect sizes were developed to normalize the outcomes of the combined studies to the same scale; this was done through the use of log response ratios (*RRs*) (Nakagawa and Santos, 2012). Variations in aerosol species were evaluated using the *RR* (Chen et al., 2015, 2017), which can be calculated as follows:

$$RR = In\left(\frac{\bar{X_P}}{\bar{X_N}}\right) = In(\bar{X_P}) - In(\bar{X_N}) \quad (1)$$

where $\bar{X_N}$ and $\bar{X_P}$ represent the mean values of the studied variables on normal and polluted days, respectively. Although most AMS/ACSM measurements cover PM_1 rather than $PM_{2.5}$, studies have mainly used $PM_{2.5}$ concentrations as the criteria for distinguishing polluted from non-polluted days (Table S2). The PM_1 mass was calculated as the sum of mass concentrations of major chemical species in the submicron aerosol, including organics, sulfate, nitrate, ammonium, chloride and black carbon.

Chen et al. (2018b) quantified $PM_1/PM_{2.5}$ ratios in China, and they found high ratios in Southeast and Central China and low ratios in Western and Northern China. We used the highest ratio reported for the cities in each region to convert the average PM_1 concentration to the $PM_{2.5}$ concentration (Table S2); hence, the converted $PM_{2.5}$ concentrations were less than or equal to the true values. Moreover, whether the converted or measured $PM_{2.5}$ concentrations were below or above the threshold value was the way in which polluted days were identified (Fig. S2). That is, days on which the daily average PM mass concentration exceeded the average (32.8–256.0 $\mu g\, m^{-3}$) were categorized as polluted days, and the remaining days were considered normal. We also conducted the meta-analysis with different threshold values (median and 75 percentile) to determine whether the results were robust (Fig. S5 and Fig. S6).

The statistical distribution of the *RR* calculated as described above was normally distributed, and only a small bias was detected (Hedges et al., 1999). Pearson correlation analysis (Sun et al., 2013b; Li et al., 2017) was used to evaluate the complex relationships between the *RR* for the OOA and meteorological parameters in each region. Based on this evaluation, the potential processing of SOA in the four regions was assessed. The data for OOA and meteorological parameters were taken from different campaign years or different sites, and therefore, relationships between the OOA and meteorological parameters may be more broadly representative of regional atmospheric processing than what is obtained from individual studies.

The effect sizes varied among the studies, and this was due to within-study (sampling) variance. The variances (v) were calculated as follows:

$$v = \frac{s_P^2}{n_P \bar{X_P}^2} + \frac{s_N^2}{n_N \bar{X_N}^2} \quad (2)$$

where n_P and n_N are the numbers of polluted days and normal days, respectively, and s_P and s_N are respectively the standard deviations of the PM concentration on the polluted and normal days. For each derived *RR*, the variance reciprocal was used as the weight (w). Furthermore, the total mean *RR* (RR_{++}) was calculated on the basis of the individual *RR* for the polluted and normal days as follows:

$$RR_{++} = \frac{\sum_{i=1}^{m}\sum_{j=1}^{k} w_{ij} RR_{ij}}{\sum_{i=1}^{m}\sum_{j=1}^{k} w_{ij}} \quad (3)$$

with m and k representing the total numbers of the compared groups and the comparisons in the analogous groups, respectively. Changes in aerosol species on the polluted days were calculated as follows:

$$[\exp(RR_{++}) - 1] \times 100\% \quad (4)$$

2.4. Uncertainties

The standard error of RR_{++} was estimated as

$$SE(RR_{++}) = \sqrt{\frac{1}{\sum_{i=1}^{m}\sum_{j=1}^{K} w_{ij}}} \quad (5)$$

The analysis was based on a fixed model using the MetaWin software (Sinauer Associates Inc., Sunderland, MA, USA), and in the model, bootstrapping was used to calculate the uncertainties for the variations in aerosol species on the polluted days. For each iteration of the model, a random choice of n studies was selected from a sample size of n with replacement. Thus, some studies would be chosen for more than once, while some studies would not be chosen at all (Rosenberg et al., 1999). This procedure was repeated numerous times to produce a measure of the spread of possible values. In the current study, the highest and lowest 2.5% values were chosen to represent the upper and lower 95% bootstrap confidence bounds, respectively (Nakagawa et al., 2017). The variations in aerosol species were considered significant if the bootstrap exhibited no overlap with zero.

3. Results

3.1. Increased secondary aerosol contributions on polluted days

In China, polluted winter days are generally characterized by enhanced secondary aerosol formation (Fig. 1). Compared with the results for normal days, the sulfate/PM mass ratio increased the most (27%) during pollution events, followed by nitrate/PM (10%) and ammonium/PM (10%) (see references listed in Table S1). The contributions of OOA to OA also were 13% higher on the polluted days.

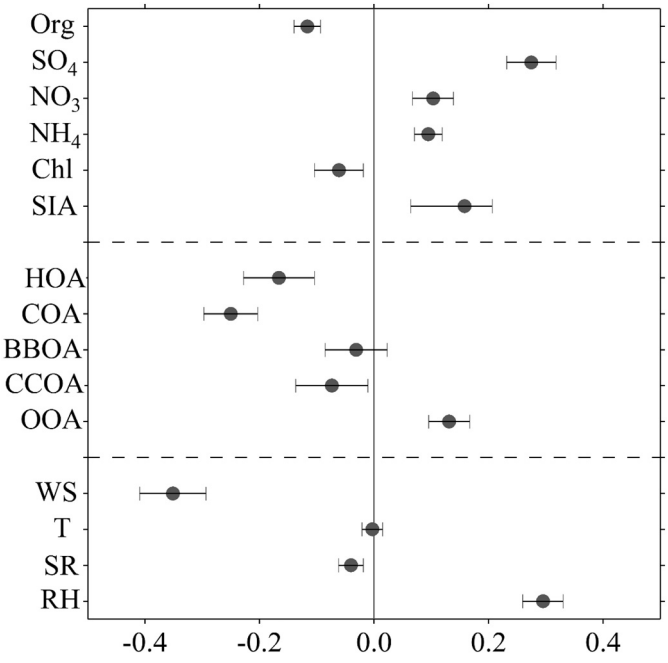

Fig. 1. Variations in aerosol composition, organic sources, and weather parameters from normal to polluted days in China during winter. The variations are considered significant if the confidence intervals of the effect size do not overlap with zero.

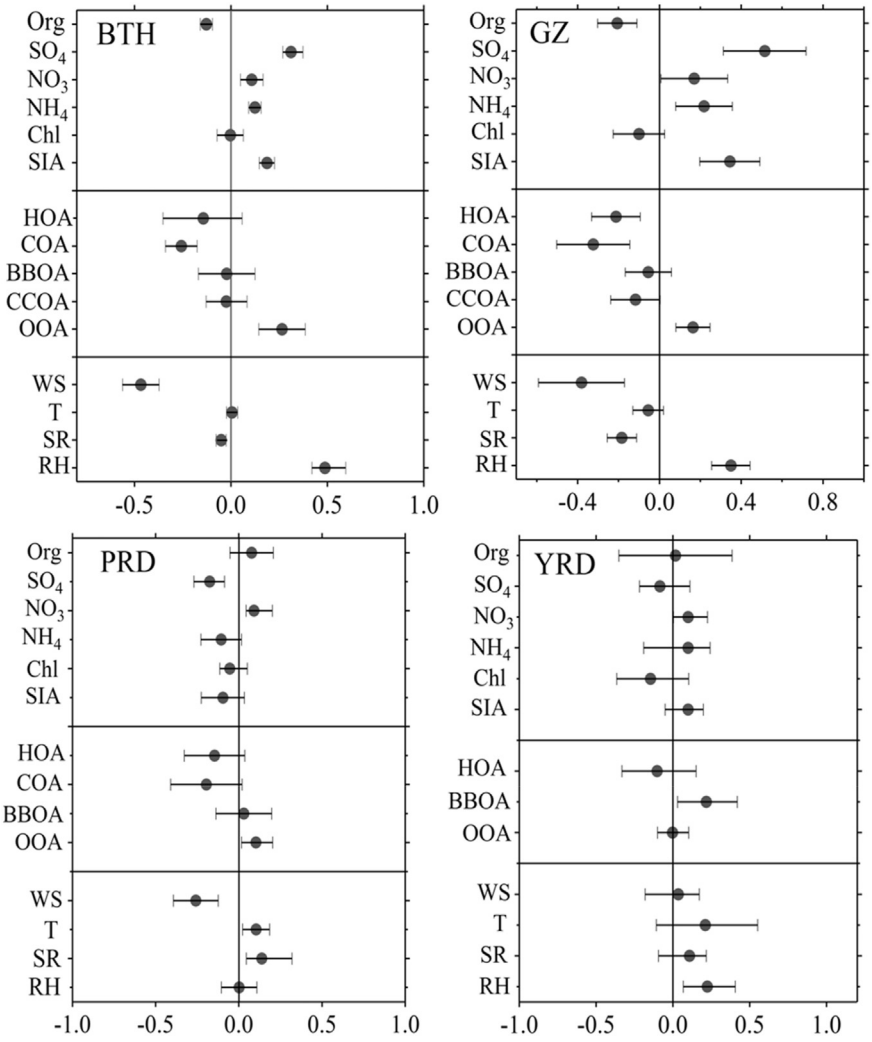

Fig. 2. Variations in aerosol composition, organic sources, and weather parameters from normal to polluted days during winter in the Beijing–Tianjin–Hebei region, Guanzhong region, Pearl River Delta region, and Yangtze River Delta region. The variations are considered significant if the confidence intervals of the effect size do not overlap with zero.

Some differences among regions were found; for example, from normal to polluted days, the contributions of OOA to total OA increased by 26%, 16%, and 10% in the BTH, GZ, and PRD regions, respectively (Fig. 2). By contrast, the proportion of BBOA relative to the total OA rose by 22% in the Yangtze River Delta (YRD) area (Fig. 2). Moreover, the fractions of total SIAs in PM increased by 19% and 34% in the BTH and GZ regions, respectively (Fig. 2). For the SIA species, the fraction of nitrate in PM increased by 9%–17% across the four regions, whereas the fraction of sulfate in PM increased in only the two Northern China regions: 27% in the BTH region and 51% in the GZ region. The PM constituents that increased on the polluted days were the same for the different threshold values used to distinguish between polluted and non-polluted days (that is, the average, median and three quarters) (Fig. S5 and Fig. S6), indicating that the results are robust.

3.2. Relationships between OOA and meteorological parameters

A positive linear relationship between OOA-RR and RH-RR was found for BTH and GZ (Fig. 3a), with a correlation coefficient (r) of 0.87 (p = 0.005, n = 11). However, OOA-RR was not correlated with SR-RR in these regions (r = 0.08, Fig. 3b). In the PRD, the OOA-RR was positively correlated with SR-RR (Fig. 3b) (r = 0.62, p = 0.20, n = 5). Moreover, the daily average mass loadings and fractions of OOA at Guangzhou and Shenzhen, two cities in the PRD, showed an overall

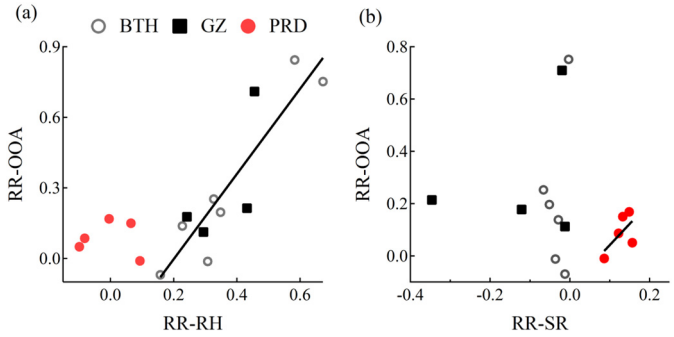

Fig. 3. Relationships between the response ratios (RRs) for OOA and weather parameters (RH and SR). The relationships for (a) RR-OOA and RR-RH in the Beijing–Tianjin–Hebei and Guanzhong regions: Y = −0.37 + 1.8×, r = 0.87, p = 0.005, n (sample number) = 11; (b) RR-OOA and RR-SR in the Pearl River Delta region: Y = −0.12 + 1.6×, r = 0.62, p = 0.2, n = 5.

parallel trend with ozone (O_3) (see Fig. S7) (Cao et al., 2018; Qin et al., 2017). Positive linear relationships between OOA and RH were seen in BTH and GZ regions when the threshold values were set to the median and 75th percentiles (Fig. S8 and Fig. S9). OOA also showed a linear relationship with SR in the PRD for the same thresholds (Fig. S8 and Fig. S9). Thus, the linear relationships appear to be robust.

4. Discussion

The results from AMS and ACSM studies were synthesized through meta-analyses, which showed that particulate pollution is driven by enhanced secondary aerosol formation in four representative regions in China during winter. A linear relationship between OOA and RH indicated that aqueous-phase reactions are likely a prime influence on OOA formation in the BTH and GZ regions. A positive correlation between OOA and SR (and with O_3) highlighted the potential importance of photochemical reactions in the PRD.

Interestingly, the combined data show that total solar radiation was less on the polluted days than on normal days in the BTH and GZ regions (Fig. 2), and therefore, the reduced solar radiation may have affected atmospheric photochemistry and oxidant concentrations (O_3 and hydroxyl radical [OH]). For example, the observations showed a decrease in the O_3 mixing ratio to < 10 ppb in the principal metropolises in the BTH area, including Beijing, Shijiazhuang, and Tianjin, on polluted days (Wang et al., 2014; Zhao et al., 2013). The model simulations indicated that [OH] decreased during pollution events in most areas of the North China Plain from 0.004 to 0.020 to 0.004 pptV (Zheng et al., 2015). As O_3 and [OH] radicals are crucial oxidants for gas-phase reactions, the intensity of photochemical reactions would be expected to decrease on polluted days in the BTH and GZ regions.

Moreover, the contributions of nitrate and sulfate rose on the polluted days in the two areas of Northern China (Fig. 2), suggesting enhancements in the secondary formation of sulfate and nitrate, most likely through heterogeneous reactions. Along these lines, Zheng et al. (2015) showed that elevated PM loadings and RH on polluted days increased the surface area and volume of aerosols, and that led to an increase in sulfate and nitrate formation and lower oxidant concentrations. In Beijing, the production of sulfate in winter was estimated to be 3.3 times higher during a pollution period with high RH and low oxidants compared with a clean period of low RH and high oxidants (Zheng et al., 2015). Chamber and model studies conducted by Wang et al. (2016) and Cheng et al. (2016) showed that NO_2 can induce the aqueous oxidation of SO_2 under high RH and NH_3 neutralization conditions. These aqueous reactions also produce nitrite, which can undergo disproportionation or oxidation reactions to form nitrate (Cheng et al., 2016).

The AMS/ACSM data for the BTH and GZ regions on polluted days showed nearly equivalent amounts of ammonium relative to the sum of sulfate, nitrate, and chloride (0.9–1.1), and therefore, the charges of the measured species were nearly in balance. The average mass concentrations of NO_x ranged from 43 to 135 ppb on polluted days during the AMS/ACSM campaigns included in our study, and this is similar to, but somewhat broader than, the ranges of NO_x (66–92 ppb) found under the polluted conditions in Beijing and Xi'an (Wang et al., 2016; Cheng et al., 2016). Therefore, SO_2 oxidation by NO_2 in the BTH and GZ regions is possibly a key mechanism leading to SIA formation on polluted days.

One would expect the aerosol liquid water content (ALWC) to be higher on polluted days than clean ones in North China because high RH and SIA loadings have been observed during those episodes (Wu et al., 2018). Increases in ALWC support the aqueous-phase formation of OOA and in so doing increase the mass concentrations and fractional contributions of these species (Ervens and Volkamer, 2010; Ervens et al., 2011; Wong et al., 2015; Wu et al., 2018; Xu et al., 2017). Organic mass concentrations are elevated on polluted days in Northern China, but solar radiation and oxidant levels are relatively low, and therefore the aqueous-phase dark reactions described by McNeill (2015) may be particularly important when pollution levels are high.

There also is evidence that lower boundary layer heights (BLHs) are associated with higher total PM mass concentrations and higher levels of various pollutants in the regions included in our study (e.g., Sun et al., 2014; Zhang et al., 2015). In addition to inhibiting the dispersion of the pollutants, decreases in BLHs can lead to increases in RH (Liu et al., 2018; Xiang et al., 2019), and this could result in the enhanced formation of secondary aerosols through aqueous-phase reactions (Ervens et al., 2011). Thus, variations in the BLH may indirectly influence the formation of secondary aerosols.

The above discussion is based on the assumption that sulfate is from the secondary processing. However, recent studies show that sulfate can be emitted directly from residential coal combustion (Dai et al., 2018, 2019). This needs to be taken into account when attempting to determine the impacts of secondary aerosols. By improving the equation from Sun et al. (2013b), we used CCOA as the tracer of coal combustion emissions and estimated the relative contribution of secondary sulfate:

$$\mathrm{Sulfate_{SF}} = \mathrm{Sulfate_{total}} - \mathrm{CCOA} \times \left(\frac{\mathrm{Sulfate}}{\mathrm{CCOA}}\right)_{\mathrm{CCE}} \quad (6)$$

where $\mathrm{sulfate_{SF}}$ refers to the sulfate associated with secondary formation. $(\mathrm{sulfate/CCOA})_{\mathrm{CCE}}$ refers to the ratio of sulfate to CCOA from coal combustion emissions and assumed to be constant throughout the observation period. Due to the negligible secondary formation of sulfate when RH < 20% at night (Zhang et al., 2015), one would expect sulfate to be mainly primary coal combustion emissions. Thus, we arbitrary selected the data that met this condition to obtain the $(\mathrm{sulfate/CCOA})_{\mathrm{CCE}}$ ratio. From Eq. (6), we found that on polluted winter days in northern China, secondary sulfate accounted for 66–97% on polluted days, indicating the total sulfate is dominated by the secondary sulfate. Moreover, the enhanced sulfate fractions from normal days to polluted days were mainly contributed by secondary sulfate (68–99%). Therefore, the influence of primary sulfate should be small in the present study.

It should be noted that OOA discussed in this study is a proxy for secondary organic aerosol (SOA). For AMS/ACSM measurements, the ion fragment m/z 44 (CO_2^+) is a major indicator for OOA, but some oxidized organics (e.g., humic-like substances, Li et al., 2018a; Tan et al., 2016) which have high m/z 44 can also be observed in primary emission sources. Even so, for the atmospheric ambient data, the primary OAs resolved by positive matrix factorization (PMF) model also contains the m/z 44 (e.g., Elser et al., 2016; Huang et al., 2019), which is attributed to the oxidative transformation of the pyrolysis products during burning process (Wang et al., 2015; Xu et al., 2016). Thus, the oxidized organics from primary emissions are apportioned into the primary organic sources during PMF analysis.

The coal burning activities are negligible in PRD region, as suggested by the low proportion of CCOA (0–2%) in OA. Thus, the sulfate in this region should be mainly from secondary processing. Sulfate was the most abundant SIA species (Cao et al., 2018; Lan et al., 2017; Qin et al., 2017), and cross-regional transport has been reported to contribute to 80% of the aerosol sulfate in the area surrounding the PRD (Lu and Fung, 2016; Wu et al., 2013). Effects of regional transport may be reduced on polluted days, as indicated by decreases in sulfate contributions. On polluted days, photochemical reactions with atmospheric oxidants degrade volatile organic compounds (VOC) and create low volatility products that can undergo gas-particle transfer to form OOA (Hallquist et al., 2009). It is possible that increased solar radiation and higher O_3 mixing ratios on polluted days promote the formation of nitrate through gas-phase photochemical reactions, leading to an increase in nitrate contributions to PM. Increased nitrate in the YRD has been ascribed to the formation and subsequent hydrolysis of N_2O_5 on polluted days (Sun et al., 2018). Increased biomass burning contributions to OA in YRD have been linked to high levoglucosan concentrations during pollution episodes (Li et al., 2018b).

The production of SOA varied among the four regions we studied, and a possible explanation for this is that there is a dimming effect caused by the high aerosol loadings in the BTH and GZ regions. This reduces atmospheric oxidant concentrations—as shown by Zheng et al. (2015) and Wang et al. (2014)—thereby decreasing photochemical reactions. Increased RH during pollution events promotes aqueous-

phase reactions, and that facilitates the formation of secondary aerosols. Compared with BTH and GZ, the PRD is characterized by relatively high temperatures and strong solar radiation; these conditions are favorable for photochemical reactions.

Our data analyses indicate that (1) increases in OOA on polluted winter days result from enhanced chemical processing and (2) that aqueous-phase reactions are relatively more important in the BTH and GZ areas and photochemical reactions in the PRD area. Finally, few AMS/ACSM studies have focused on the aerosol characteristics in suburban and rural areas during winter (Table S1). This data gap should be filled in the future, and in particular, more information needs to be obtained on the regional characteristics of secondary aerosols.

5. Conclusions

The conclusions of this study are as follows:

- Secondary aerosol fractions increased during particulate pollution events in China during winter; on polluted days, the observed mass fractions of sulfate, nitrate and ammonium in PM increased by 10%–27%, and the mass fractions of OOA in OA increased by 13%.
- All secondary inorganic aerosol species (sulfate, nitrate and ammonium) increased in the BTH and GZ areas, but only nitrate increased in the PRD and YRD regions.
- The organic sources increased during the pollution events but differed across the regions: BBOA increased in the YRD area, whereas OOA formation increased in the other three areas.
- The increased SOA production was due to the aqueous-phase processing in the BTH and GZ regions while photochemical reactions were more important in the PRD area.
- Future AMS/ACSM observations should focus on the aerosol characteristics in rural areas during winter in China.

Acknowledgments

The National Natural Science Foundation of China supported this work (Nos. 71804115, and 21661132005), as did the China Postdoctoral Science Foundation (No. 2018M640809) and Open Fund of the State Key Laboratory of Loess and Quaternary Geology (SKLLQG1834). Qiyuan Wang also acknowledged the support of the Key Research and Development Program of Shaanxi Province and the Youth Innovation Promotion Association CAS. The authors gratefully acknowledged the NOAA Air Resources Laboratory (ARL) for providing the solar radiation data (http://www.ready.noaa.gov) and the World Meteorological Organization (WMO) for the provision of weather data used in this publication.

Appendix A. Supplementary data

Supplementary data to this article can be found online at https://doi.org/10.1016/j.envint.2019.03.021.

References

Banerjee, T., Murari, V., Kumar, M., Raju, M.P., 2015. Source apportionment of airborne particulates through receptor modeling: Indian scenario. Atmos. Res. 164, 167–187.
Button, K.S., Ioannidis, J.P.A., Mokrysz, C., Nosek, B., Flint, J., Robinson, E.S.J., Munafo, M.R., 2013. Power failure: why small sample size undermines the reliability of neuroscience. Nat. Rev. Neurosci. 14, 1–12.
Cao, L.M., Huang, X.F., Li, Y.Y., Hu, M., He, L.Y., 2018. Volatility measurement of atmospheric submicron aerosols in an urban atmosphere in southern China. Atmos. Chem. Phys. 18, 1729–1743.
Chen, G., Morawska, L., Zhang, W., Li, S., Cao, W., Ren, H., Wang, B., Wang, H., Knibbs, L., Williams, G., Guo, J., Guo, Y., 2018b. Spatiotemporal variation of PM_1 pollution in China. Atmos. Environ. 178, 198–205.
Chen, J., Luo, Y., Van Groenigen, K.J., Hungate, B.A., Cao, J., Zhou, X., Wang, R.W., 2018a. A keystone microbial enzyme for nitrogen control of soil carbon storage. Sci. Adv. 4.
Chen, J., Luo, Y., Xia, J.Y., Jiang, L.F., Zhou, X.H., Lu, M., Liang, J.Y., Shi, Z., Shelton, S., Cao, J.J., 2015. Stronger warming effects on microbial abundances in colder regions. Sci. Rep. 5, 18032.
Chen, J., Luo, Y.Q., Li, J.W., Zhou, X.H., Cao, J.J., Wang, R.W., Wang, Y.Q., Shelton, S., Jin, Z., Walker, L.M., Feng, Z.Z., Niu, S.L., Feng, W.T., Jian, S.Y., Zhou, L.Y., 2017. Costimulation of soil glycosidase activity and soil respiration by nitrogen addition. Glob. Chang. Biol. 23, 1328–1337.
Cheng, Y., Zheng, G., Wei, C., Mu, Q., Zheng, B., Wang, Z., Gao, M., Zhang, Q., He, K., Carmichael, G., 2016. Reactive nitrogen chemistry in aerosol water as a source of sulfate during haze events in China. Sci. Adv. 2, e1601530.
Dai, Q., Bi, X., Liu, B., Li, L., Ding, J., Song, W., Bi, S., Schulze, B., Song, C., Wu, J., Zhang, Y., Feng, Y., Philip, H., 2018. Chemical nature of $PM_{2.5}$ and PM_{10} in Xi'an, China: insights into primary emissions and secondary particle formation. Environ. Pollut. 240, 155–166.
Dai, Q., Bi, X., Song, W., Li, T., Liu, B., Ding, J., Xu, J., Song, C., Yang, N., Schulze, B.C., Zhang, Y., Feng, Y., Hopke, P., 2019. Residential coal combustion as a source of primary sulfate in Xi'an, China. Atmos. Environ. 196, 66–76.
Duplissy, J., DeCarlo, P.F., Dommen, J., Alfarra, M.R., Metzger, A., Barmpadimos, I., Prevôt, A.S.H., Weingartner, E., Tritscher, T., Gysel, M., Aiken, A.C., Jimenez, J.L., Canagaratna, M.R., Worsnop, D.R., Collins, D.R., Tomlinson, J., Baltensperger, U., 2011. Relating hygroscopicity and composition of organic aerosol particulate matter. Atmos. Chem. Phys. 11, 1155–1165.
Elser, M., Huang, R.-J., Wolf, R., Slowik, J.G., Wang, Q., Canonaco, F., Li, G., Bozzetti, C., Daellenbach, K.R., Huang, Y., Zhang, R., Li, Z., Cao, J., Baltensperger, U., El-Haddad, I., Prévôt, A.S.H., 2016. New insights into $PM_{2.5}$ chemical composition and sources in two major cities in China during extreme haze events using aerosol mass spectrometry. Atmos. Chem. Phys. 16, 3207–3225.
Ervens, B., Turpin, B.J., Weber, R.J., 2011. Secondary organic aerosol formation in cloud droplets and aqueous particles (aqSOA): a review of laboratory, field and model studies. Atmos. Chem. Phys. 11 (21), 11069–11102.
Ervens, B., Volkamer, R., 2010. Glyoxal processing by aerosol multiphase chemistry: towards a kinetic modeling framework of secondary organic aerosol formation in aqueous particles. Atmos. Chem. Phys. 10 (17), 8219–8244.
Fontes, T., Li, P.L., Barros, N., Zhao, P.J., 2017. Trends of $PM_{2.5}$ concentrations in China: a long term approach. J. Environ. Manag. 196, 719–732.
Fu, H., Chen, J., 2017. Formation, features and controlling strategies of severe haze-fog pollutions in China. Sci. Total Environ. 578, 121–138.
Fuzzi, S., Baltensperger, U., Carslaw, K., Decesari, S., Denier van der Gon, H., Facchini, M.C., Gilardoni, S., 2015. Particulate matter, air quality and climate: lessons learned and future needs. Atmos. Chem. Phys. 15, 8217–8299.
Glass, G.V., 1976. Primary, secondary, and meta-analysis of research. Educ. Res. 5, 3–8.
Gurevitch, J., Koricheva, J., Nakagawa, S., Stewart, G., 2018. Meta-analysis and the science of research synthesis. Nature 555, 175–182.
Hallquist, M., Wenger, J.C., Baltensperger, U., Rudich, Y., Simpson, D., Claeys, M., Dommen, J., Donahue, N.M., George, C., Goldstein, A.H., Hamilton, J.F., Herrmann, H., Hoffmann, T., Iinuma, Y., Jang, M., Jenkin, M.E., Jimenez, J.L., Kiendler-Scharr, A., Maenhaut, W., McFiggans, G., Mentel, T., Monod, A., Prevót, A.S.H., Seinfeld, J.H., Surratt, J.D., Szmigielski, R., Wildt, J., 2009. The formation, properties and impact of secondary organic aerosol: current and emerging issues. Atmos. Chem. Phys. 9, 5155–5236.
Hartikainen, A., Yli-Pirila, P., Tiitta, P., Leskinen, A., Kortelainen, M., Orasche, J., Schnelle-Kreis, J., Lehtinen, K.E.J., Zimmermann, R., Jokiniemi, J., Sippula, O., 2018. Volatile organic compounds from logwood combustion: emissions and transformation under dark and photochemical aging conditions in a smog chamber. Environ. Sci. Technol. 52, 4979–4988.
Hedges, L.V., 1994. Research synthesis as a scientific enterprise. In: The Handbook of of Research Synthesis. vol. 236. pp. 3.
Hedges, L.V., Gurevitch, J., Curtis, P.S., 1999. The meta-analysis of response ratios in experimental ecology. Ecology 80, 1150–1156.
Hu, W., Hu, M., Hu, W., Jimenez, J.L., Yuan, B., Chen, W., Wang, M., Wu, Y., Chen, C., Wang, Z., Peng, J., Zeng, L., Shao, M., 2016. Chemical composition, sources and aging process of submicron aerosols in Beijing: contrast between summer and winter. J. Geophys. Res. 121, 1955–1977.
Hu, W., Hu, M., Hu, W.W., Zheng, J., Chen, C., Wu, Y.S., Guo, S., 2017. Seasonal variations in high time-resolved chemical compositions, sources, and evolution of atmospheric submicron aerosols in the megacity Beijing. Atmos. Chem. Phys. 17, 9979–10000.
Huang, R.-J., Wang, Y., Cao, J., Lin, C., Duan, J., Chen, Q., Li, Y., Gu, Y., Yan, J., Xu, W., Fröhlich, R., Canonaco, F., Bozzetti, C., Ovadnevaite, J., Ceburnis, D., Canagaratna, M.R., Jayne, J., Worsnop, D.R., El-Haddad, I., Prévôt, A.S.H., O'Dowd, C.D., 2019. Primary emissions versus secondary formation of fine particulate matter in the top polluted city, Shijiazhuang, in North China. Atmos. Chem. Phys. 19, 2283–2298.
Huang, R.-J., Zhang, Y.L., Bozzetti, C., Ho, K.-F., Cao, J.J., Han, Y.M., Daellenbach, K.R., Slowik, J.G., Platt, S.M., Canonaco, F., Zotter, P., Wolf, R., Pieber, S.M., Bruns, E.A., Crippa, M., Ciarelli, G., Piazzalunga, A., Schwikowski, M., Abbaszade, G., Schnelle-Kreis, J., Zimmermann, R., An, Z., Szidat, S., Baltensperger, U., Haddad, I.E., Prévôt, A.S.H., 2014. High secondary aerosol contribution to particulate pollution during haze events in China. Nature 514, 218–222.
Jimenez, J.L., Canagaratna, M.R., Donahue, N.M., Prévôt, A.S.H., Zhang, Q., Kroll, J.H., DeCarlo, P.F., Allan, J.D., Coe, H., Ng, N.L., Aiken, A.C., Docherty, K.S., Ulbrich, I.M., Grieshop, A.P., Robinson, A.L., Duplissy, J., Smith, J.D., Wilson, K.R., Lanz, V.A., Hueglin, C., Sun, Y.L., Tian, J., Laaksonen, A., Raatikainen, T., Rautiainen, J., Vaattovaara, P., Ehn, M., Kulmala, M., Tomlinson, J.M., Collins, D.R., Cubison, M.J., Dunlea, E.J., Huffman, J.A., Onasch, T.B., Alfarra, M.R., Williams, P.I., Bower, K., Kondo, Y., Schneider, J., Drewnick, F., Borrmann, S., Weimer, S., Demerjian, K., Salcedo, D., Cottrell, L., Griffin, R., Takami, A., Miyoshi, T., Hatakeyama, S., Shimono, A., Sun, J.Y., Zhang, Y.M., Dzepina, K., Kimmel, J.R., Sueper, D., Jayne,

J.T., Herndon, S.C., Trimborn, A.M., Williams, L.R., Wood, E.C., Middlebrook, A.M., Kolb, C.E., Baltensperger, U., Worsnop, D.R., 2009. Evolution of organic aerosols in the atmosphere. Science 326, 1525–1529.
Lan, Z., Zhang, B., Huang, X., Zhu, Q., Yuan, J., Zeng, L., Hu, M., He, L., 2017. Source apportionment of $PM_{2.5}$ light extinction in an urban atmosphere in China. J. Environ. Sci. 63, 277–284.
Lanz, V.A., Alfarra, M.R., Baltensperger, U., Buchmann, B., Hueglin, C., Prevó t, A.S.H., 2007. Source apportionment of submicron organic aerosol at an urban site by factor analytical modeling of aerosol mass spectra. Atmos. Chem. Phys. 7 (6), 1503–1522.
Lanz, V.A., PrevóT, A.S.H., Alfarra, M.R., Weimer, S., Mohr, C., DeCarlo, P.F., Gianini, M.F.D., Hueglin, C., Schneider, J., Favez, O., D'Anna, B., George, C., Baltensperger, U., 2010. Characterization of aerosol chemical composition with aerosol mass spectrometry in Central Europe: an overview. Atmos. Chem. Phys. 10 (21), 10453–10471.
Lelieveld, J., Evans, J.S., Fnais, M., Giannadaki, D., Pozzer, A., 2015. The contribution of out-door air pollution sources to premature mortality on a global scale. Nature 525, 367–371.
Li, X., Han, J., Hopke, P.K., Hu, J., Shu, Q., Chang, Q., 2019a. Quantifying primary and secondary humic-like substances in urban aerosol based on emission source characterization and a source-oriented air quality model. Atmos. Chem. Phys. 19, 2327–2341.
Li, Y.J., Sun, Y., Zhang, Q., Li, X., Li, M., Zhou, Z., Chan, C.K., 2017. Real-time chemical characterization of atmospheric particulate matter in China: a review. Atmos. Environ. 158, 270–304.
Li, Z., Li, C., Ye, X., Fu, H., Wang, L., Yang, X., Wang, X., Zhao, Z., Kan, H., Mellouki, A., Chen, J., 2018b. Air quality in the middle and lower reaches of the Yangtze River channel: a cruise campaign. Atmos. Chem. Phys. 18, 14445–14464.
Liu, Q., Jia, X., Quan, J., Li, J., Li, X., Wu, Y., Chen, D., Wang, Z., Liu, Y., 2018. New positive feedback mechanism between boundary layer meteorology and secondary aerosol formation during severe haze events. Sci. Rep. 8, 6095.
Lu, X., Fung, J.C.H., 2016. Source apportionment of sulfate and nitrate over the Pearl River Delta region in China. Atmosphere 7, 98–110.
McNeill, V.F., 2015. Aqueous organic chemistry in the atmosphere: sources and chemical processing of organic aerosols. Environ. Sci. Technol. 49, 1237–1244.
Nakagawa, S., Noble, D.W.A., Senior, A.M., Lagisz, M., 2017. Meta evaluation of meta-analysis: ten appraisal questions for biologists. BMC Biol. 15, 18.
Nakagawa, S., Santos, E.S.A., 2012. Methodological issues and advances in biological meta-analysis. Evol. Ecol. 26, 1253–1274.
Pratt, K.A., Prather, K.A., 2012. Mass spectrometry of atmospheric aerosols–recent developments and applications. Part II: on-line mass spectrometry techniques. Mass Spectrom. Rev. 31, 17–48.
Qin, Y.M., Tan, H.B., Li, Y.J., Schurman, M.I., Li, F., Canonaco, F., Prévôt, A.S.H., Chan, C.K., 2017. Impacts of traffic emissions on atmospheric particulate nitrate and organics at a downwind site on the periphery of Guangzhou, China. Atmos. Chem. Phys. 17, 10245–10258.
Rosenberg, M.S., Adams, D.C., Gurevitch, J., 1999. MetaWin: Statistical Software for Meta-Analysis. Version 2.0. Sinauer Associates, Sunderland, Massachusetts.
Sun, P., Nie, W., Chi, X., Xie, Y., Huang, X., Xu, Z., Qi, X., Xu, Z., Wang, L., Wang, T., Zhang, Q., Ding, A., 2018. Two years of online measurement of fine particulate nitrate in the western Yangtze River Delta: influences of thermodynamics and N_2O_5 hydrolysis. Atmos. Chem. Phys. 18, 17177–17190.
Sun, Y.L., Du, W., Wang, Q., Zhang, Q., Chen, C., Chen, Y., Chen, Z., Fu, P., Wang, Z., Gao, Z., Worsnop, D.R., 2015. Real-time characterization of aerosol particle composition above the urban canopy in Beijing: insights into the interactions between the atmospheric boundary layer and aerosol chemistry. Environ. Sci. Technol. 49, 11340–11347.
Sun, Y.L., Jiang, Q., Wang, Z.F., Fu, P.Q., Li, J., Yang, T., Yin, Y., 2014. Investigation of the sources and evolution processes of severe haze pollution in Beijing in January 2013. J. Geophys. Res. Atmos. 119 (7), 4380–4398.
Sun, Y.L., Wang, Z., Fu, P., Jiang, Q., Yang, T., Li, J., Ge, X., 2013b. The impact of relative humidity on aerosol composition and evolution processes during wintertime in Beijing, China. Atmos. Environ. 77, 927–934.
Sun, Y.L., Wang, Z.F., Fu, P.Q., Yang, T., Jiang, Q., Dong, H.B., Li, J., Jia, J.J., 2013a. Aerosol composition, sources and processes during wintertime in Beijing, China. Atmos. Chem. Phys. 13, 4577–4592.
Tan, J.H., Xiang, P., Zhou, X.M., Duan, J.C., Ma, Y.L., He, K.B., Cheng, Y., Yu, J.Z., Querol, X., 2016. Chemical characterization of humic-like substances (HULIS) in $PM_{2.5}$ in Lanzhou, China. Sci. Total Environ. 573, 1481–1490.
Tao, J., Zhang, L., Cao, J., Zhang, R., 2017. A review of current knowledge concerning $PM_{2.5}$ chemical composition, aerosol optical properties and their relationships across China. Atmos. Chem. Phys. 17, 9485–9518.
Viana, M., Kuhlbusch, T.A.J., Querol, X., Alastuey, A., Harrison, R.M., Hopke, P.K., et al., 2008. Source apportionment of particulate matter in Europe: a review of methods and results. J. Aerosol Sci. 39, 827–849.
Walser, M.L., Desyaterik, Y., Laskin, J., Laskin, A., Nizkorodov, S.A., 2008. High-resolution mass spectrometric analysis of secondary organic aerosol produced by ozonation of limonene. Phys. Chem. Chem. Phys. 10, 1009–1022, 2008.
Walser, M.L., Park, J., Gomez, A.L., Russell, A.R., Nizkorodov, S.A., 2007. Photochemical aging of secondary organic aerosol particles generated from the oxidation of d-limonene. J. Phys. Chem. A 111, 1907–1913.
Wang, G., Zhang, R., Gomez, M.E., Yang, L., Zamora, M.L., Hu, M., 2016. Persistent sulfate formation from London Fog to Chinese haze. Proc. Natl. Acad. Sci. U. S. A. 113, 13630–13635.
Wang, Q., Elser, M., Huang, R.J., Liu, S.X., Wang, Y.C., Haddad, I.E., Prévôt, A.S.H., Cao, J.J., 2017b. Real-time characterization of aerosol particle composition during winter high-pollution events in China. In: Air Pollution in Eastern Asia: An Integrated Perspective. Springer, Cham, pp. 221–244.
Wang, X.F., Cotter, E., Iyer, K.N., Fang, J.X., Williams, B.J., Biswas, P., 2015. Relationship between pyrolysis products and organic aerosols formed during coal combustion. Proc. Combust. Inst. 35, 2347–2354.
Wang, Y., Yao, L., Wang, L., Liu, Z., Ji, D., Tang, G., Zhang, J., Sun, Y., Hu, B., Xin, J., 2014. Mechanism for the formation of the January 2013 heavy haze pollution episode over central and eastern China. Sci. China Earth Sci. 57, 14–25.
Wang, Y.C., Huang, R.J., Ni, H.Y., Chen, Y., Wang, Q.Y., Li, G.H., Tie, X.X., Shen, Z.X., Huang, Y., Liu, S.X., 2017a. Chemical composition, sources and secondary processes of aerosols in Baoji City of Northwest China. Atmos. Environ. 158, 128–137.
Wong, J.P.S., Lee, A.K.Y., Abbatt, J.P.D., 2015. Impacts of sulfate seed acidity and water content on isoprene secondary organic aerosol formation. Environ. Sci. Technol. 49 (22), 13215–13221.
Wu, D., Fung, J.C.H., Yao, T., Lau, A.K.H., 2013. A study of control policy in the Pearl River Delta region by using the particulate matter source apportionment method. Atmos. Environ. 76, 147–161.
Wu, Z., Wang, Y., Tan, T., Zhu, Y., Li, M., Shang, D., Wang, H., Lu, K., Guo, S., Zeng, L., Zhang, Y., 2018. Aerosol liquid water driven by anthropogenic inorganic salts: implying its key role in haze formation over the North China plain. Environ. Sci. Tech. Let. 5, 160–166.
Xiang, Y., Zhang, T., Liu, J., Lv, L., Dong, Y., Chen, Z., 2019. Atmosphere boundary layer height and its effect on air pollutants in Beijing during winter heavy pollution. Atmos. Res. 215, 305–316.
Xu, J., Shi, J., Zhang, Q., Ge, X., Canonaco, F., Prévôt, A.S.H., Vonwiller, M., Szidat, S., Ge, J., Ma, J., An, Y., Kang, S., Qin, D., 2016. Wintertime organic and inorganic aerosols in Lanzhou, China: sources, processes, and comparison with the results during summer. Atmos. Chem. Phys. 16, 14937–14957.
Xu, W., Han, T., Du, W., Wang, Q., Chen, C., Zhao, J., Zhang, Y., Li, J., Fu, P., Wang, Z., Worsnop, D.R., Sun, Y., 2017. Effects of aqueous phase and photochemical processing on secondary organic aerosol formation and evolution in Beijing, China. Environ. Sci. Technol. 51 (2), 762–770.
Zhang, J.K., Cheng, M.T., Ji, D.S., Liu, Z.R., Hu, B., Sun, Y., Wang, Y.S., 2016a. Characterization of submicron particles during biomass burning and coal combustion periods in Beijing. Sci. Total Environ. 562, 812–821.
Zhang, J.K., Sun, Y., Liu, Z.R., Ji, D.S., Hu, B., Liu, Q., Wang, Y.S., 2014b. Characterization of submicron aerosols during a month of serious pollution in Beijing, 2013. Atmos. Chem. Phys. 14 (6), 2887–2903.
Zhang, Q., He, K.B., Huo, H., 2012. Cleaning China's air. Nature 484, 161–162.
Zhang, Q., Jimenez, J.L., Canagaratna, M.R., Allan, J.D., Coe, H., Ulbrich, I., Alfarra, M.R., Takami, A., Middlebrook, A.M., Sun, Y.L., Dzepina, K., Dunlea, E., Docherty, K., DeCarlo, P.F., Salcedo, D., Onasch, T., Jayne, J.T., Miyoshi, T., Shimono, A., Hatakeyama, S., Takegawa, N., Kondo, Y., Schneider, J., Drewnick, F., Borrmann, S., Weimer, S., Demerjian, K., Williams, P., Bower, K., Bahreini, R., Cottrell, L., Griffin, R.J., Rautiainen, J., Sun, J.Y., Zhang, Y.M., Worsnop, D.R., 2007. Ubiquity and dominance of oxygenated species in organic aerosols in anthropogenically-influenced Northern Hemisphere midlatitudes. Geophys. Res. Lett. 34, L13801.
Zhang, R., Wang, G., Guo, S., Zamora, M.L., Ying, Q., Lin, Y., Wang, W., Hu, M., Wang, Y., 2015. Formation of urban fine particulate matter. Chem. Rev. 115, 3803–3855.
Zhang, X., Schwantes, R.H., Coggon, M.M., Loza, C.L., Schilling, K.A., Flagan, R.C., Seinfeld, J.H., 2014a. Role of ozone in SOA formation from alkane photooxidation. Atmos. Chem. Phys. 14 (3), 1733–1753.
Zhang, Y., Cai, J., Wang, S., He, K., Zheng, M., 2017. Review of receptor-based source apportionment research of fi M particulate matter and its challenges in China. Sci. Total Environ. 586, 917–929.
Zhang, Y., Sun, Y., Du, W., Wang, Q., Chen, C., Han, T., Lin, J., Zhao, J., Xu, W., Gao, J., 2016b. Response of aerosol composition to different emission scenarios in Beijing, China. Sci. Total Environ. 571, 902–908.
Zhao, X.J., Zhao, P.S., Xu, J., Meng, W., Pu, W.W., Dong, F., He, D., Shi, Q.F., 2013. Analysis of a winter regional haze event and its formation mechanism in the North China Plain. Atmos. Chem. Phys. 13, 5685–5696.
Zheng, G.J., Duan, F.K., Su, H., Ma, Y.L., Cheng, Y., Zheng, B., Zhang, Q., Huang, T., Kimoto, T., Chang, D., Pöschl, U., Cheng, Y.F., He, K.B., 2015. Exploring the severe winter haze in Beijing: the impact of synoptic weather, regional transport and heterogeneous reactions. Atmos. Chem. Phys. 15, 2969–2983.